

# Seismic Retrofit of Shear Walls with Headed Bars and Carbon Fiber Wrap

James Paterson<sup>1</sup> and Denis Mitchell, M.ASCE<sup>2</sup>

**Abstract:** A series of four shear wall specimens was tested in order to evaluate the seismic retrofit that had been proposed for the core wall of an existing building. The core wall had nonductile reinforcing details, including lap splices in the longitudinal reinforcement in potential plastic hinging regions, inadequate confinement of boundary regions, and inadequate anchorage of the transverse reinforcement. The seismic retrofit involved the use of headed reinforcement, carbon fiber wrap, and reinforced concrete collars at the base of the wall. The four shear wall specimens were tested under reversed cyclic loading. Two of these walls had a lap splice in the longitudinal steel at the base of the wall, and the other two had a lap splice 600 mm from the base of the wall. One of each of these specimens was tested in the as-built condition and the other two were retrofit prior to testing. The test results show that the retrofit strategies were successful in improving the ductility and energy dissipation of the shear walls.

**DOI:** 10.1061/(ASCE)0733-9445(2003)129:5(606)

**CE Database subject headings:** Retrofitting; Seismic design; Shear walls; Concrete, reinforced; Reinforcement; Confinement; Shear strength.

## Introduction

This paper describes research on the seismic retrofit of reinforced concrete shear walls that was undertaken to investigate a proposed retrofit for an existing building in Berkeley, California (Mar et al. 2000). The core wall of this building was designed and constructed in the 1960's and, therefore, does not meet current design and detailing standards. In order to achieve ductile response, all brittle failure modes must be avoided and the energy should be dissipated by the formation of plastic hinges, typically at the base of the wall. In regions of potential plastic hinges, the boundary elements must be adequately confined and bar buckling must be prevented through the use of closely spaced hoops around the concentrated vertical reinforcement. Lap splices should not be located in plastic hinge regions, since they limit the extent of yielding and can also suffer from bond degradation under the cyclic loading. Also, the shear strength of the wall must be greater than the shear associated with the formation of plastic hinging at the base of the wall.

The core wall of this existing building has a number of design and detailing deficiencies, including lap splices in the longitudinal reinforcement at locations of plastic hinging, poor confinement of the boundary element reinforcement, poor anchorage of the transverse reinforcement, and insufficient shear strength to develop

hinging. Retrofit strategies included the use of carbon fiber wrap, headed pins, and headed reinforcing bars.

Carbon fiber wrap has been used successfully for the retrofit of bridge columns. Priestley et al. (1996) have recommended design and detailing requirements for fiber wrapping. Seible et al. (1997) and Pantelides et al. (1999) demonstrated the effectiveness of composite material jacket retrofits for confining lap splices, increasing shear strength, and improving concrete confinement in columns. Griezic et al. (1996) demonstrated retrofit techniques for lap splices involving strengthening the cross section to move the plastic hinge away from the lap splice. Berner et al. (1999) described seismic applications of headed bars in bridge structures.

## Objective

The objective of these tests is to determine the effectiveness of the combined use of headed reinforcement, carbon fiber wrap, and the addition of reinforced concrete collars on the retrofit of older walls. The goal of the retrofit is to improve the system ductility and overall energy absorption of the poorly detailed walls.

## Test Program

The research program involved the construction and testing of four shear wall specimens. Two of the specimens were tested in the as-built condition, and two companion walls were retrofit prior to testing. Specimen W1R was the retrofit companion specimen of W1 and W2R was the retrofit companion specimen of W2.

Fig. 1(a) shows the critical region in the existing core wall that would be subjected to very high tensile and compressive strains under reversed cyclic loading. Fig. 1(b) shows the locations of the lap splices in the vertical reinforcing bars just above the level of the floor slabs. The test specimens were chosen to simulate this critical region containing the lap splices.

The walls were tested in the horizontal position, cantilevered out from a heavily reinforced foundation block that was anchored

<sup>1</sup>Structural Engineer, Weidlinger Associates Incorporated, One Broadway, 11th Floor, Cambridge, MA 02142.

<sup>2</sup>Professor, Dept. of Civil Engineering and Applied Mechanics, McGill Univ., 817 Sherbrooke St. W., Montreal PQ, Canada H3A 2K6. E-mail: denis.mitchell@mcgill.ca

Note. Associate Editor: Joseph M. Bracci. Discussion open until October 1, 2003. Separate discussions must be submitted for individual papers. To extend the closing date by one month, a written request must be filed with the ASCE Managing Editor. The manuscript for this paper was submitted for review and possible publication on October 16, 2001; approved on August 16, 2002. This paper is part of the *Journal of Structural Engineering*, Vol. 129, No. 5, May 1, 2003. ©ASCE, ISSN 0733-9445/2003/5-606-614/\$18.00.

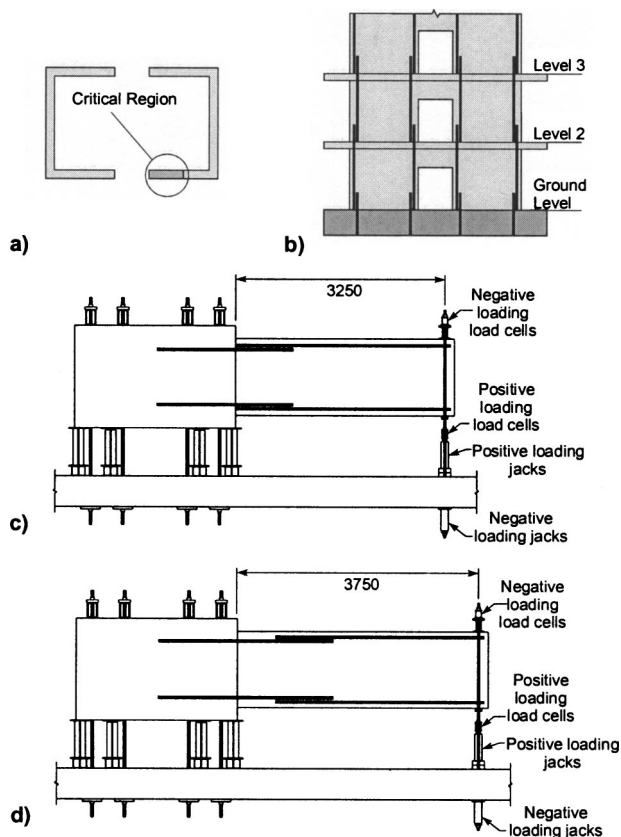


**Fig. 1.** As-built shear wall and test setup: (a) Typical core wall section; (b) Typical core wall elevation showing lap splices above floor levels; (c) Test setup, lap splice at wall base; and (d) test setup, lap splice 600 mm from wall base

to a strong floor. Reversed cyclic loading was applied 150 mm from the tip of the wall by hydraulic jacks using the strong floor for reaction [Figs. 1(c and d)]. Each cycle of the loading consisted of positive (pushing up on the tip of the wall) and negative loading. Three reversed cycles were done at each load/deflection level. The specimens were cycled to selected load levels, at a loading rate of about 15 kN/min, up until general yielding occurred. After general yielding the specimens were cycled to multiples of the yield deflection, at a deflection rate of about 4 mm/min.

At the positive and negative peaks of each cycle, testing was stopped to take photographs and measure crack widths. During loading, data were collected by load cells, linear voltage differential transformers (LVDTs), and strain gauges on the reinforcing steel, headed reinforcement, and carbon fiber wrap. A potentiometer was used to measure the tip deflection of the specimen. For specimens W1, W2, and W2R, horizontal LVDTs were placed at the base of the wall parallel to the longitudinal reinforcement. These LVDTs measured displacements over a length of 50 mm, enabling the curvature to be determined at this critical location. The strains obtained from the LVDTs were supplemented with strains obtained from the strain gauges. For specimen W1R, the critical section occurs at the top of the reinforced concrete collar and, hence, the horizontal LVDTs at this location (with a gauge length of 400 mm) were used to determine the curvature. In Fig. 1, illustrating the responses of the specimens, the locations of the LVDT's used to determine the curvatures and the locations of the strain gauges are indicated.

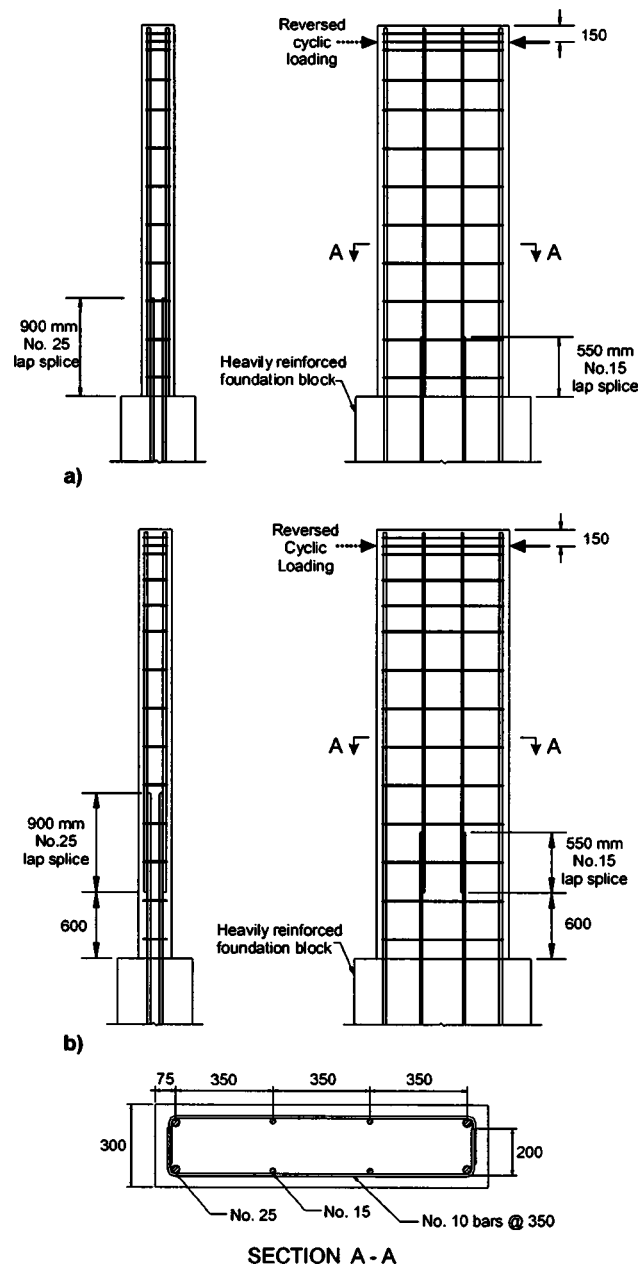


**Fig. 2.** Specimen details: (a) Specimen W1 and (b) Specimen W2

### As-Built Specimens W1 and W2

Specimens W1 and W2 were tested in the as-built condition. They were detailed to simulate the critical region of the existing core wall that required retrofit. The two as-built test specimens model the presence of lap splices at various floor levels. Specimen W1 was designed and constructed with a lap splice at the base of the wall [Fig. 1(c)]. This is intended to model the situation where the lap splice occurs at the base of the structure. Specimen W2 was designed and constructed with a lap splice beginning  $d/2$  (or 600 mm) from the base of the wall [Fig. 1(d)]. This specimen simulates the situation where a lap splice is present just above a region of flexural hinging, as would be the case at the second or third floor level of the structure after retrofit.

### Design and Construction of Specimens W1 and W2

The cross section of the as-built specimens was detailed to have similar dimensions and properties to the critical section of the

**Table 1.** Concrete Material Properties

Specimen	Batch	$f'_c$ , (MPa)	$\epsilon'_c$ , (mm/mm)	$f_r$ , (MPa)	$f_{sp}$ , (MPa)
W1	Wall	25.9	0.0020	3.99	2.35
W1R	Wall	26.1	0.0020	3.99	2.35
W1R	Reinforced concrete collar	29.9	0.0021	4.78	—
W2	Wall	33.4	0.0022	4.14	3.05
W2R	Wall	31.0	0.0021	4.63	2.55

existing core wall. The concentrated reinforcement at each end of the wall consists of two No. 25 bars (bar area=500 mm<sup>2</sup>) and the distributed reinforcement (No. 15 bars, bar area=200 mm<sup>2</sup>) were chosen in order to achieve a similar yield force to the reinforcing bars in the as-built structure. The areas of the bars were factored down by the ratio of the yield forces between the existing wall and the test specimen. The dimensions and the reinforcing bar sizes for the as-built specimens are shown in section A-A of Fig. 2.

The transverse steel consists of No. 10 bars (bar area=100 mm<sup>2</sup>) at 350 mm spacing and was chosen to provide a shear-critical wall specimen. In addition, the transverse reinforcement in the wall was anchored by 90° hooks at the ends of the wall to simulate the poor details in the existing structure. The lap splices in the existing core wall are approximately 24 times the bar diameter; this was a typical lap splice length at the time that the wall was constructed. In order to account for the higher strength of steel, the lap splice lengths were factored up by the ratio of the steel yield forces. The lap splice lengths in the test specimens are, therefore, approximately 35 times the bar diameter. The lengths and positions of the lap splices are shown in Figs. 2(a) and (b).

The strength of the concrete used in the wall specimens was relatively low in order to be similar to the concrete in the existing core wall. The material properties of the concrete and the reinforcing steel for the specimens are summarized in Tables 1 and 2.

### Performance of Specimen W1

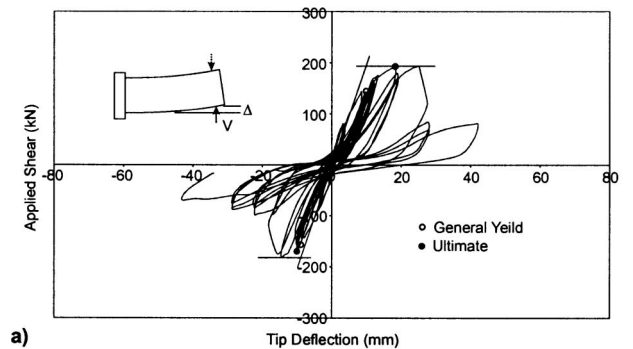
The performance of specimen W1 is described in Fig. 3. This specimen exhibited very poor ductility, as it failed soon after yielding. There was a brittle failure of the lap splices of the No. 25 bars at the base of the wall that led to a significant drop in capacity. This lap splice failure, made evident by the longitudinal cracks along the lap splices, can be seen in Fig. 3(c).

The displacement ductility of specimen W1 was determined from the load versus tip deflection plot [Fig. 3(a)]. For each of the walls, the general yield deflection ( $\Delta_y$ ) was determined using the secant stiffness of the response (Park 1989). The ultimate deflec-

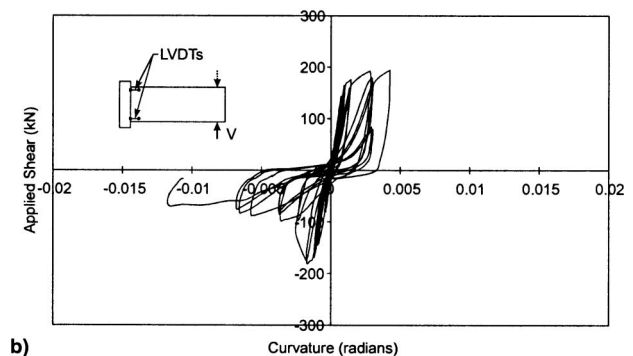
tion ( $\Delta_u$ ) was defined to be the maximum deflection at which the wall could endure three load cycles without the capacity dropping below 80% of the maximum load. The displacement ductility for specimen W1 was only 1.5 and there was almost no increase in strength or displacement after general yielding. The hysteretic loops are very pinched, and there is a large drop in capacity after the ultimate displacement is reached. The predicted nominal flexural resistance, neglecting any strain hardening, is 644.5 kNm. The wall reached a shear of 193.7 kN, corresponding to an applied moment of 629.5 kNm or 98% of the predicted flexural capacity.

Strain gauges that were placed on the dowel reinforcement at the base of the wall indicated that there was a small amount of localized yielding at this section. The strains remained elastic in the lap splice region, as the effective area of steel was higher. This resulted in a very short plastic hinge length.

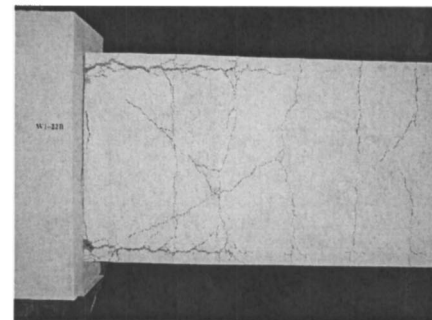
The shape of the curvature response of specimen W1 for the section at the base of the wall [Fig. 3(b)] was similar to the shape of the load versus deflection plot, indicating very little inelastic action after yield.



a)



b)



c)

**Fig. 3.** Response of specimen W1: (a) Shear versus tip deflection; (b) Shear versus curvature at base; and (c) Photo at end of testing

**Table 2.** Reinforcing Steel Material Properties

Bar	Area (mm <sup>2</sup> )	$f_y$ (MPa)	$\epsilon_y$ (mm/mm)	$f_u$ (MPa)
No. 10	100	320	0.0022	459
No. 15	200	453	0.0020	709
No. 25	500	423	0.0022	667
No. 5 (U.S.) headed bar	200	483	0.0026	687
17 mm diameter rod (one end headed and one end threaded)	227	595	0.0024	743

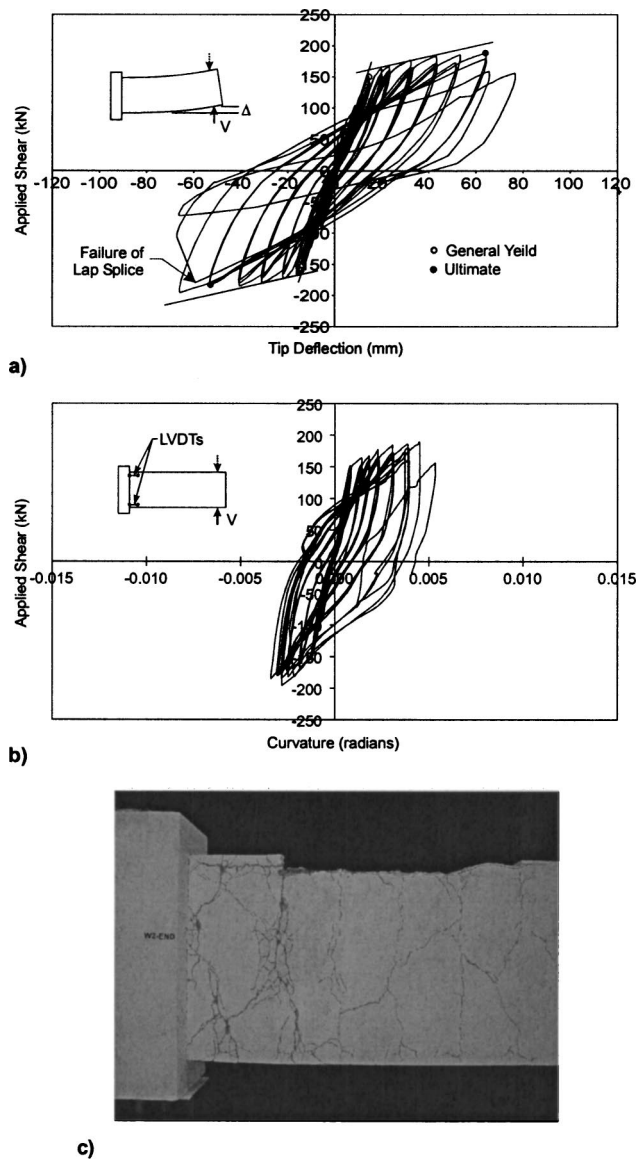


**Fig. 4.** Response of specimen W2: (a) Shear versus tip deflection; (b) Shear versus curvature at base; and (c) Photo at end of testing

### Performance of Specimen W2

Specimen W2 exhibited a surprisingly ductile response [Fig. 4], especially considering the poor design details that were used. The lap splices in the main flexural reinforcement and in the uniformly distributed steel were at a location where considerable shear distress and flexural hinging would occur. There was a large amount of inelastic action at the base of the wall that was indicated by cracking and damage in this area [Fig. 4(c)]. A brittle tensile failure of the lap splice on one side of the specimen eventually resulted in a large drop in the capacity of this specimen. The specimen exhibited considerable ductility due to the delayed failure of the lap splice. The lap splice did not exhibit any significant distress until flexural hinging spread into the splice region. The maximum shear reached in the wall was 189.1 kNm, corresponding to a moment of 614.6 kNm (96% of the flexural capacity).

The displacement ductility for specimen W2 was relatively high, at 4.0. The large hysteretic loops on the load versus tip deflection response [Fig. 4(a)] indicate that the response was ductile.

There was considerable strength reserve, as the strength continued to increase until the lap splice failed on the second negative loop, cycled to approximately five times the yield displacement. The curvature response for the section at the base of the wall [Fig. 4(b)] showed good hysteretic behavior, indicating a large amount of plastic hinging.

Strain gauges on the longitudinal steel indicated that the highest strains were at base of wall, with yielding of the longitudinal bars extending well into the lap splice. As a result, the length of hinging was over 1000 mm.

### Retrofit Specimens W1R and W2R

Retrofit strategies involving the use of headed reinforcement and carbon fiber wrap were employed to improve the seismic performance of the wall specimens. Companion walls to W1 and W2 were cast and had identical details. The concrete strengths were slightly different between the specimens due to the increase in strength over time (see Table 1). Wall W1R simulated a retrofit for the situation when a lap splice is located at the base of the wall, while W2R simulated a retrofit strategy for the situation when a lap splice occurs at a higher level.

#### Retrofit of Specimen W1R

The retrofit of specimen W1R involved strengthening the lap splice at the base of the wall by adding a reinforced concrete collar [Fig. 5(a)]. This collar extended the full length of the lap splice (900 mm) and served to move the plastic hinge to a location above the lap splice. Headed reinforcement was used in this collar in order to develop the yield strength of the steel in the small amount of space available. Four No. 5 (bar area = 199 mm<sup>2</sup>) headed dowels that were epoxy grouted into the foundation blocks on each side of the wall acted as longitudinal reinforcement in the collar. Additional headed reinforcement was provided in the transverse and through-wall directions to offer confinement to the headed dowels. The headed reinforcement placed in holes drilled through the wall was designed such that the collar would act compositely with the wall. The dimensions and the details of this lap splice retrofit are shown in Fig. 5(a) and Section A-A of Fig. 5. Fig. 6(a) shows the headed reinforcement in the reinforced concrete collar prior to casting.

Over the entire height of the wall, the confinement in the end regions was improved by grouting headed reinforcement end pins into holes that had been drilled into the wall. These pins served to improve the confinement of the 90° hooks which anchored the transverse reinforcement (see Fig. 5).

Above the concrete collar, the shear strength of the wall was increased by applying carbon fiber wrap. The carbon fiber wrap was applied in strips and was designed to increase the shear strength to a level necessary to develop plastic hinging without suffering shear failure. In order to test the effectiveness of the carbon fiber wrap, it was designed to be on the limit of the shear strength required, while in actual retrofits, a greater reserve of shear strength would be provided. The through-wall headed reinforcement was provided to increase confinement and to assist in anchoring the carbon fiber wrap.

The photograph in Fig. 6(b) shows a closeup of the retrofit of the wall above the concrete collar, showing the carbon fiber strips and the heads of the through-wall headed reinforcement and end pins. The details of the retrofit for this portion of the wall are shown in section B-B of Fig. 5.

The material properties of the headed reinforcing bars and pins are given in Table 2. The friction welds connecting the heads to

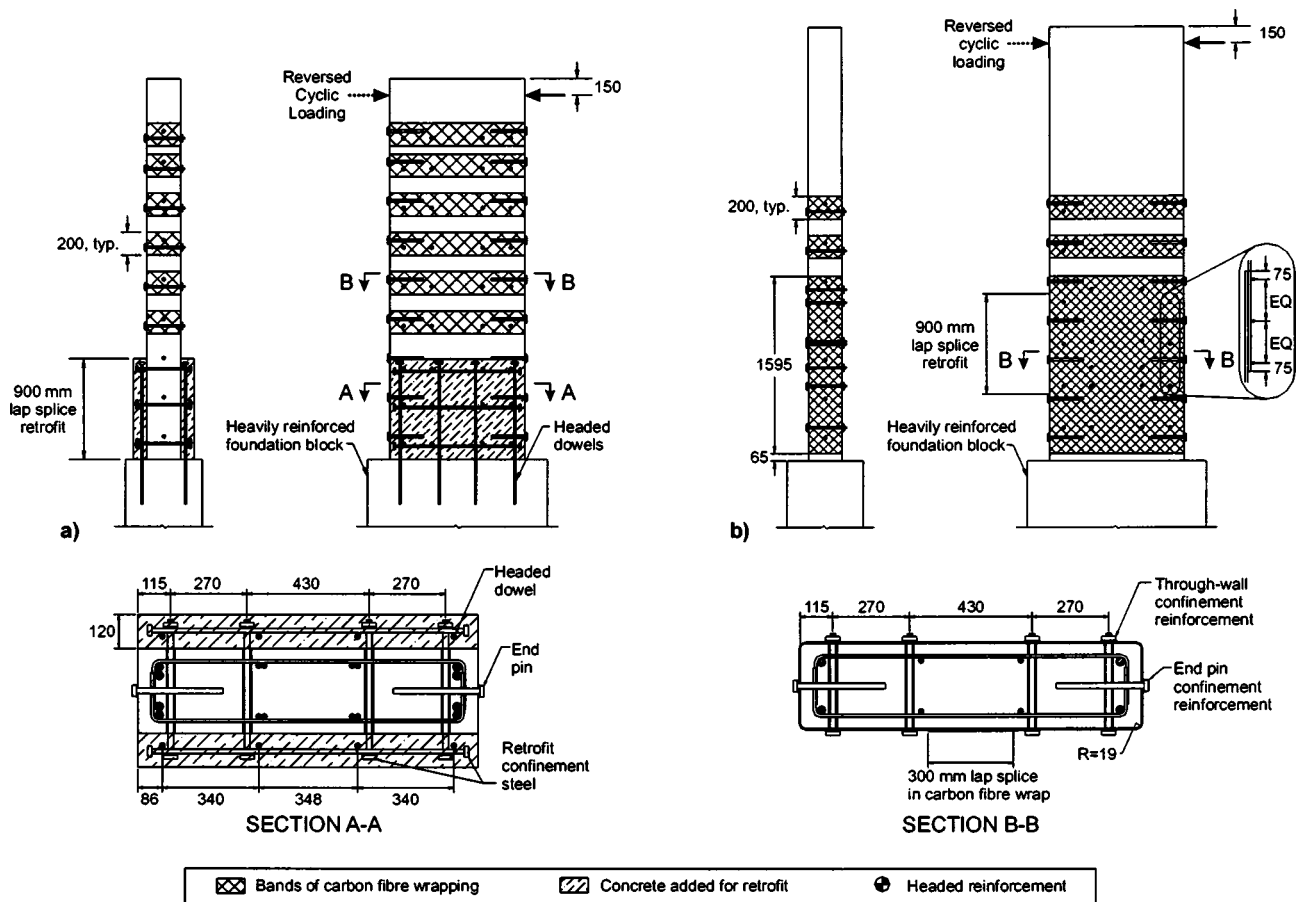


**Fig. 5.** Retrofit details: (a) Specimen W1R and (b) Specimen W2R

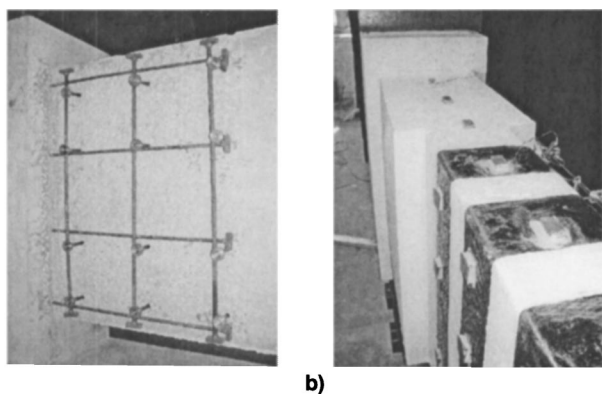
the headed reinforcement were capable of developing the ultimate strength of the bar. The 17 mm diameter through-wall reinforcement had threaded heads on one end in order to allow them to pass through holes drilled in the wall, with the strength of these bars being governed by the strength of the threads. The reinforced concrete collar was constructed with a different batch of concrete from that of the wall, the properties of this concrete are described in Table 1. In the direction parallel to the strips, the carbon fiber wrap had an ultimate strength of 876 N per millimeter width and

had a rupture strain of 1.26% (Tyfo® 2000). The carbon fiber wrap has no strength in the direction perpendicular to the strips.

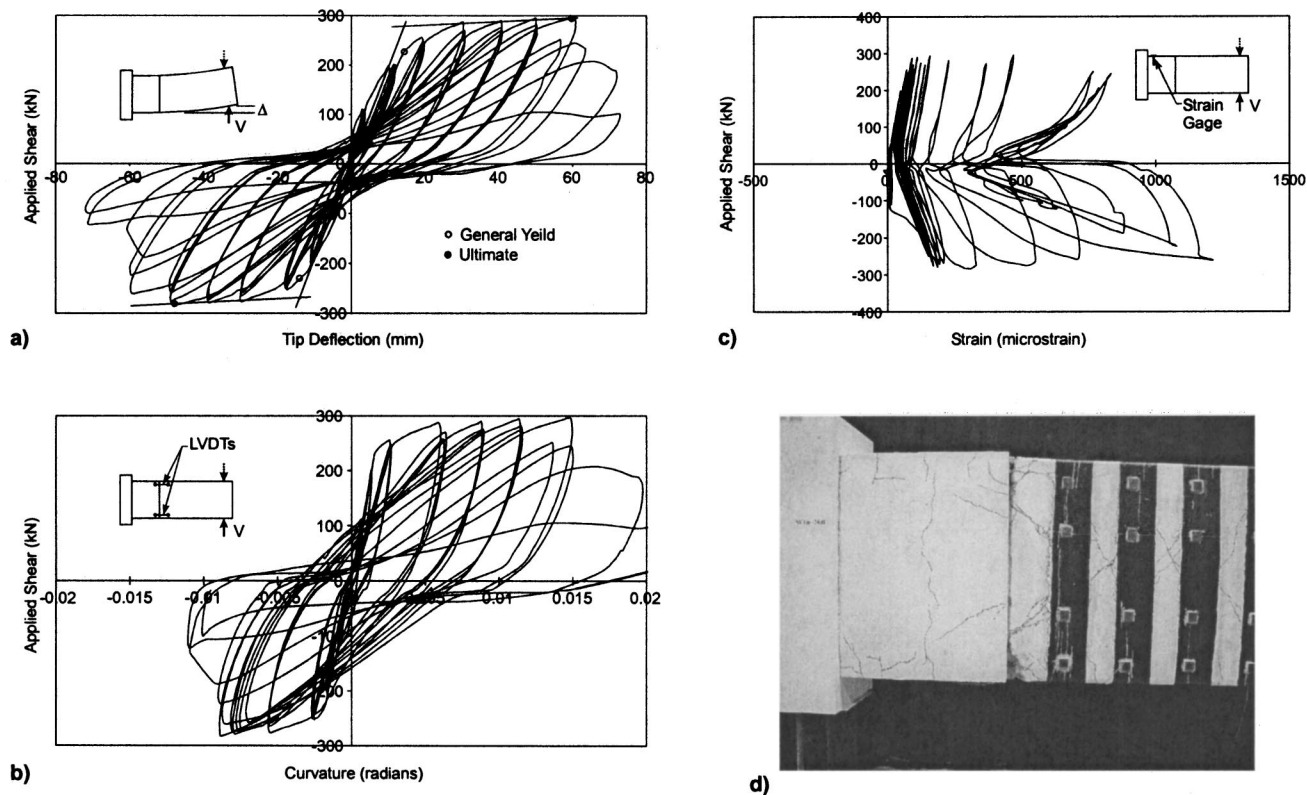
### Performance of Specimen W1R

Fig. 7 illustrates the response of specimen W1R. The lap splice retrofit succeeded in moving the flexural hinge to the portion of the wall above the reinforced concrete collar. The load versus deflection response for specimen W1R [Fig. 7(a)] shows a very ductile response, with a displacement ductility of 3.8. The hysteresis loops were large, indicating that a significant amount of energy was absorbed. There was a large reserve of strength after general yielding, with the resistance of the wall gradually degrading due to crushing of the concrete just above the reinforced concrete collar. The curvature response for this critical region [Fig. 7(b)] shows that there was a large amount of flexural hinging at this location. There was also a small amount of flexural hinging at the base of the wall. For this specimen, the critical section has been shifted from the base of the wall to a location 2350 mm from the loading point. The maximum applied shear was 296.3 kN giving a maximum moment of 696.3 kNm at the critical section. This maximum moment is 8% above the predicted yield moment, indicating that considerable flexural hinging took place.

The strains in the longitudinal steel indicated that there was significant yielding in the longitudinal reinforcement in the section of the wall above the retrofit collar. The length of this plastic hinge was approximately 950 mm. Some yielding of the longitu-



**Fig. 6.** Details of retrofit specimens: (a) Headed reinforcing bars for concrete collar at base of specimen W1R and (b) Grouted end pins and through-wall pins at carbon fiber wrap bands



**Fig. 7.** Response of specimen W1R: (a) Shear versus tip deflection; (b) Shear versus curvature at top of reinforced concrete collar; (c) Strain in end pin at base of wall; and (d) Photo at end of testing

dinal reinforcement and headed dowels at the base of the wall indicated that there was a small amount of inelastic action at this section.

Fig. 7(c) shows the shear versus strain response of the end pin closest to the base of the wall. This plot indicates that this pin was active in the prevention of spalling, as the strain was gradually increasing as the damage to the wall increased.

The carbon fiber wrap was effective in increasing the shear strength of the wall as well as adding to the confinement of the longitudinal reinforcement. The strains in the carbon fiber wrap reached 3,100 microstrain in locations where the wrap was acting to confine splitting along the longitudinal reinforcement.

Fig. 7(d) shows the appearance of the specimen at the end of testing. The large cracks and concrete crushing indicate the significant inelastic action that occurred in the region above the reinforced concrete collar.

### Retrofit of Specimen W2R

The retrofit of specimen W2R involved strengthening the wall using headed reinforcement and carbon fiber wrap to increase the confinement and shear strength. Since the lap splice was not at the base of the wall it was decided to provide additional confinement over the lap splice instead of using a reinforced concrete collar. The plastic hinge would remain at the base of the wall (as for W2), but with the lap splice better confined, degradation of the splice under cyclic loading could be reduced.

The lap splices in both the No. 15 and No. 25 bars were confined using a combination of carbon fiber wrap and passive through-the-wall headed bars. Three of these headed bars were placed adjacent to the splice over the length of the lap splice; the placement of these bars is shown in Fig. 5(b). A typical retrofit

cross section for specimen W2R is shown in section B-B of Fig. 5. Since the carbon fiber wrap also served to confine the lap splice, the wrap was applied to the entire length of the lap splice.

The carbon fiber wrap over the lap splice was extended to the base of the wall. Through-wall headed bars and headed pins were added as indicated in Fig. 5(b). In the region above the lap splice, strips of carbon fiber wrap were used together with headed pins and through-wall headed bars to improve confinement and increase the shear strength. The material properties of the headed reinforcement and the carbon fiber wrap were the same as those for specimen W1R.

### Performance of Specimen W2R

The load versus tip deflection response for specimen W2R [Fig. 8(a)] displays excellent hysteretic loops, indicating a large amount of energy absorption and flexural yielding. There was a large amount of strength and displacement reserve after general yielding, with the specimen achieving a displacement ductility of 6.3. Failure of the lap splice was prevented throughout the test, with the wall finally losing its load carrying ability when one of the longitudinal bars ruptured in low-cycle fatigue at the base of the wall. The curvature response at the base of the wall is shown in Fig. 8(b). This plot shows that there was a large amount of inelastic flexural action at this section, and a large amount of energy dissipated. The maximum shear reached was 202.3 kN and the corresponding moment at the base of the wall was 657.5 kNm. It is clear that significant flexural yielding took place in this specimen.

The strains in the longitudinal steel indicate that the length of the plastic hinge at the base of the wall was approximately 860 mm. Yielding did not extend as far into the lap splice region as it

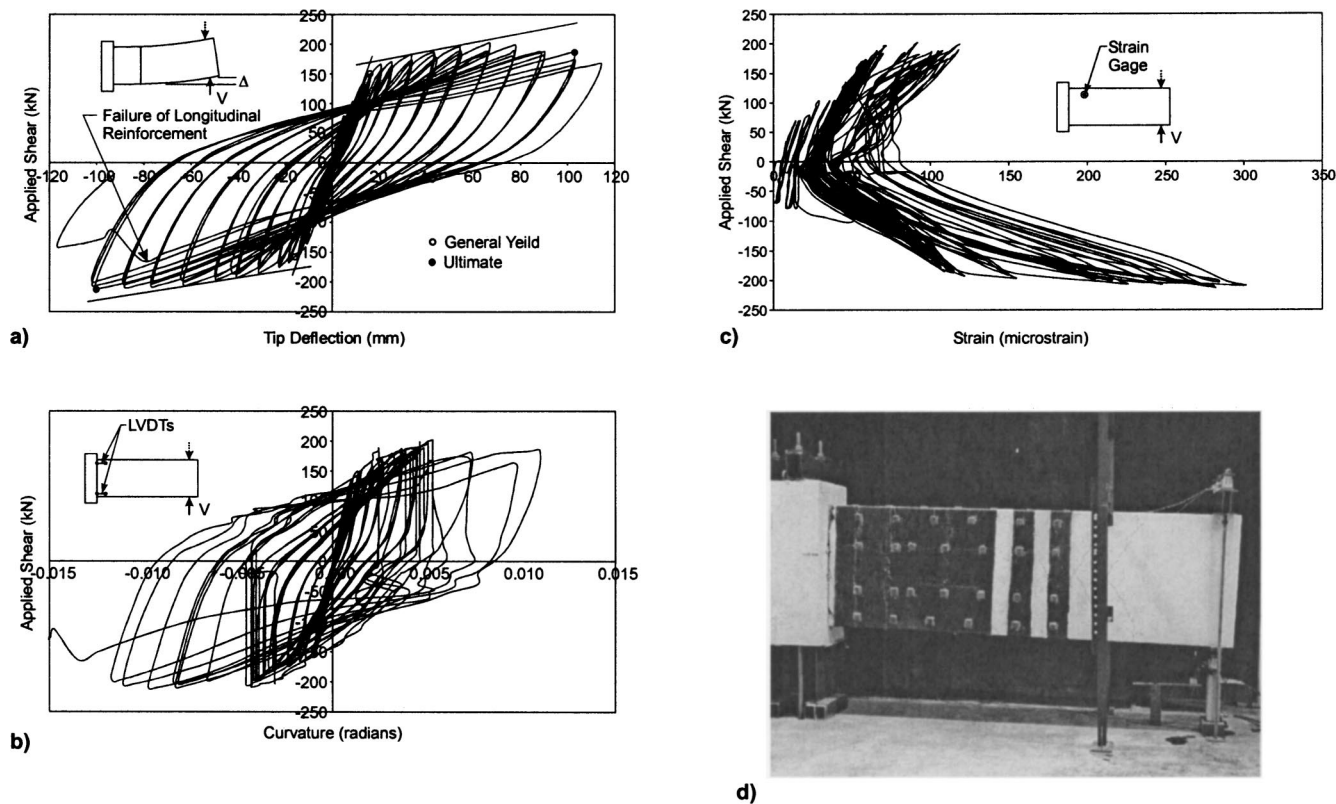


**Fig. 8.** Response of specimen W2R: (a) Shear versus tip deflection; (b) Shear versus curvature at base; (c) Strain in end pin at base of wall; and (d) Photo at end of testing

did for specimen W2, as the confined lap splice was more effective in developing the reinforcement. This resulted in a shorter plastic hinge than that for W2, but the specimen was more ductile since the confinement of the lap splice prevented bond failure.

The action of the through-wall headed reinforcement is demonstrated by the shear versus strain response for the bar at the base of the lap splice [Fig. 8(c)]. The strains in this bar are low (below 300 microstrain), but it can be seen that the strain in the bar increases with increasing damage to the wall. Also, the strains are much higher for the negative loading cycles, when the adjacent longitudinal lap splice is in tension.

The strains in the carbon fiber wrap were highest closest to the base of the wall, where the wrap was primarily providing confinement. The distress of the carbon fiber wrap at this location was made evident by tension failures and separation between the wrap and the wall. Adjacent to the lap splices of the No. 25 bars, the strains in the carbon fiber wrap were low, but increased when the lap splice was in tension. A photograph of the wall after the testing is presented in Fig. 8(d).

### Effectiveness of Retrofits

The hysteretic responses of the as-built and retrofit specimens were compared by using load versus displacement responses, displacement ductilities, load sustainability, and cumulative energy dissipated. The load sustainability after yield is represented by the load sustainability ratio  $V_u/V_y$  where  $V_u$  is the ultimate shear and  $V_y$  is the yield shear. Fig. 9 shows the load ratio ( $V/V_y$ ) versus the ductility level ( $\Delta/\Delta_y$ ) for the four specimens. In the plot of Fig. 9, the shears are taken as the average values from the positive

and negative loading cycles, and all three cycle peaks are shown at each ductility level. The bandwidth between the first and third cycles is an indicator of the degradation in load carrying capability between these cycles. The cumulative energy dissipated is the total area of the hysteretic loops on the load versus deflection responses. Fig. 10 compares the cumulative energy dissipated for the four specimens.

### Comparison of W1 and W1R

Comparison of the load versus tip deflection responses for specimens W1 and W1R [Figs. 3(a) and 7(a)] indicate the improved performance of W1R compared to W1. The hysteretic loops for specimen W1 were highly pinched and the specimen barely made it into the inelastic range prior to the brittle failure of the lap splice. The hysteretic loops of specimen W1R were much larger and the failure mode (flexural yielding in plastic hinge) of the specimen was much more ductile.

The deflection ductility of W1R was 3.8, while the as-built specimen, W1, had a deflection ductility of 1.5. This increase shows that there was a large improvement in the ductility of the specimen.

The load sustainability ratios ( $V_u/V_y$ ) for specimens W1 and W1R are 1.18 and 1.26, respectively, indicating a higher increase in strength after yielding for the retrofit specimen. Fig. 9(a) shows the superior performance of specimen W1R compared to specimen W1. With W1R exhibiting greater ductility, a smaller bandwidth, and a greater increase in strength after yield. Fig. 10(a) shows that specimen W1R dissipated over seven times as much energy as specimen W1, with specimen W1 dissipating 21 kNm and specimen W1R dissipating 151 kNm.

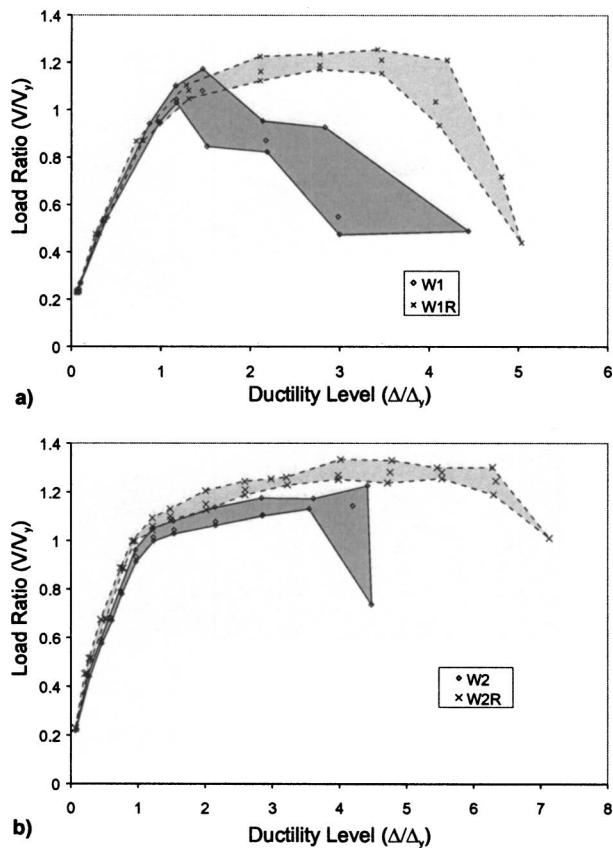


**Fig. 9.** Load ratio versus ductility: (a) Specimens W1 and W1R and (b) Specimens W2 and W2R

### Comparison of W2 and W2R

The load versus tip deflection responses for specimens W2 [Fig. 4(a)] and W2R [Fig. 8(a)] both indicated very ductile responses, with similar behavior up to a deflection of about 50 mm. At this deflection level, the lap splice in specimen W2 failed in a brittle manner, the capacity of the wall dropped off suddenly, and the hysteresis loops became much more pinched. Wall W2R continued to exhibit ductile behavior well after a deflection of 50 mm, reaching a deflection of 100 mm before one of the longitudinal reinforcing bars failed in low-cycle fatigue.

The deflection ductility for specimen W2R was 6.3, while the deflection ductility for W2 was 4.0. This increase indicates a significantly more ductile response in the retrofit specimen.

Fig. 9(b) illustrates the improved overall response of specimen W2R beyond a displacement ductility level of 4.0. Both specimens exhibited a narrow bandwidth, indicating that there was little decay of stiffness upon cycling up to a ductility level of 4.0. The load sustainability ratio for specimen W2R was 1.31, which is somewhat better than the load sustainability ratio of 1.18 for specimen W2. As shown in Fig. 10(b), specimen W2R absorbed over three times as much energy as specimen W2, with W2R dissipating 384 kNm in hysteretic damping and W2 dissipating 126 kNm.

### Conclusions

Specimens W1 and W1R represented the situation where there are lap splices in the longitudinal reinforcement at the base of the wall. Specimen W1 had a very low ductility with the lap splice

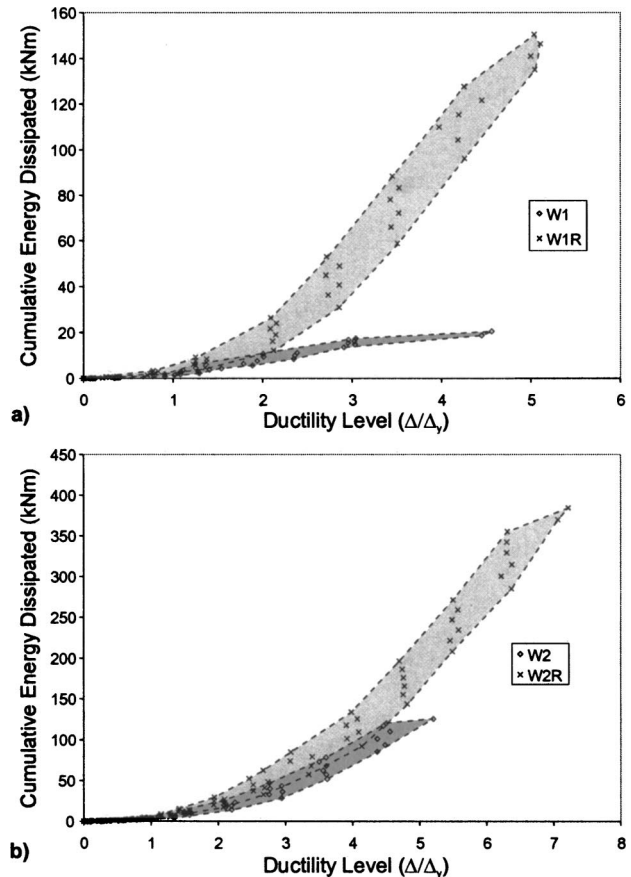


**Fig. 10.** Cumulative energy dissipated versus ductility: (a) Specimens W1 and W1R and (b) Specimens W2 and W2R

failing in a brittle manner soon after yield. The reinforced concrete collar retrofit of specimen W1R was effective in strengthening the lap splice region moving the plastic hinge to a location above the reinforced concrete collar. As a result of this retrofit, the displacement ductility was increased from 1.5 to 3.8 and the retrofit specimen absorbed over seven times as much energy as specimen W1.

Specimen W2 and W2R had a lap splice in the longitudinal reinforcement that started 600 mm from the base of the wall. Both of these specimens had a relatively ductile response, but the lap splice in the as-built specimen broke down under cyclic loading when yielding spread into the lap splice. This eventually led to a brittle failure of the splice. The retrofit of specimen W2R was effective in providing confinement for the lap splice and preventing bond failure under cyclic loading. The retrofit of specimen W2R increased the displacement ductility from 4.0 to 6.3, and the retrofit specimen absorbed three times as much energy as the as-built specimen.

The combination of the headed reinforcement and the carbon fiber wrap was shown to be effective in increasing the confinement of the wall boundary element regions and the anchorage of the transverse reinforcement. The carbon fiber wrap was also effective in reducing the shear distress in the test specimens.

### Acknowledgments

The writers gratefully acknowledge Kjell and Christian Dahl of Headed Reinforcement Corporation (HRC) for providing the

headed bars and Fyfe Co. LLC for providing the carbon fiber wrap. Thanks are extended to David Mar and Leo Panian of Tipping Mar & Associates for their useful collaboration and discussions. The writers acknowledge the generous funding provided by the National Science and Engineering Research Council of Canada (NSERC) through the Strategic Projects Grant Program and the Postgraduate Scholarships Program.

## References

- Berner, D., Dahlgren, T., and Dahl, K. (1999). "Design and detailing with headed reinforcement for seismically resistant concrete bridge structures." *ACI SP-184*, Development of Seismic Steel Products and Systems, ACI, Detroit, 23–43.
- Griezic, A., Cook, W. D., and Mitchell, D. (1996). "Seismic retrofit of bridge column-footing connections." *Proc., 11th World Conf. on Earthquake Engineering (CD-ROM)*, Paper No. 508, 1–8, International Association for Earthquake Engineering, Acapulco.
- Mar, D., et al. (2000). "Performance-based seismic upgrade of a 14-story suspended slab building using state-of-the-art analysis and construction techniques." *Proc., 69th Annual Structural Engineers Assoc. of California Convention*, SEAOC, Oakland, Calif., 1–12.
- Pantelides, C. P., Gergely, J., Reaveley, L. D., and Volnyy, V. A. (1999). "Retrofit of RC bridge pier with CFRP advanced composites." *J. Struct. Eng.*, 125(10), 1094–1099.
- Park, R. (1989). "Evaluation of ductility of structures and structural assemblages from laboratory testing." *Bull. New Zealand Nat. Soc. for Earthquake Eng.*, 22(3), 155–166.
- Priestley, M. J. N., Seible, F., and Calvi, G. M. (1996). *Seismic design and retrofit of bridges*, Wiley, New York.
- Seible, F., Priestley, M. J. N., Hegemier, G. A., and Innamorato, D. (1997). "Seismic retrofit of RC columns with continuous carbon fiber jackets." *J. Compos. Constr.*, 1(2), 52–62.
- "Tyfo® SCH-35 Composite." (2000). (<http://www.fyfeco.com/SCH-35%20comp.pdf>) (Aug. 13, 2001).